ISSN 1674-1056
http://cpb.iphy.ac.cn
http://iopscience.iop.org/cpb
中国物理 B
Chinese Physics
中国物理 Chinese Physics B

A simple method to synthesize worm-like AlN nanowires and its field emission studies

Qi Liang(梁琦), Meng-Qi Yang(杨孟骐), Chang-Hao Wang(王长昊), and Ru-Zhi Wang(王如志)

Citation: Chin. Phys. B, 2021, 30 (**8**): 087302. DOI: 10.1088/1674-1056/abe3e7
Journal homepage: http://cpb.iphy.ac.cn; http://iopscience.iop.org/cpb

What follows is a list of articles you may be interested in

Growth mechanism of atomic-layer-deposited TiAlC metal gatebased on $TiCl_4$ and TMA precursors

Jinjuan Xiang(项金娟), Yuqiang Ding(丁玉强), Liyong Du(杜立永), Junfeng Li(李俊峰),Wenwu Wang(王文武), Chao Zhao(赵超)

Chin. Phys. B, 2016, 25 (**3**): 037308. DOI: 10.1088/1674-1056/25/3/037308

Controllable synthesis of ultrathin vanadium oxide nanobelts via an EDTA-mediated hydrothermal process

Yu-Xiang Qin(秦玉香), Cheng Liu(刘成), Wei-Wei Xie(谢威威), Meng-Yang Cui(崔梦阳)

Chin. Phys. B, 2016, 25 (**2**): 027307. DOI: 10.1088/1674-1056/25/2/027307

AlGaN/GaN high electron mobility transistorwith Al_2O_3+BCB passivation

Zhang Sheng, Wei Ke, Yu Le, Liu Guo-Guo, Huang Sen, Wang Xin-Hua, Pang Lei, Zheng Ying-Kui, Li Yan-Kui, Ma Xiao-Hua, Sun Bing, Liu Xin-Yu

Chin. Phys. B, 2015, 24 (**11**): 117307. DOI: 10.1088/1674-1056/24/11/117307

Growth mechanism and modification of electronic and magnetic properties of silicene

Liu Hong-Sheng, Han Nan-Nan, Zhao Ji-Jun

Chin. Phys. B, 2015, 24 (**8**): 087303. DOI: 10.1088/1674-1056/24/8/087303

Topological structure effect on far-infrared spectra in a GaAs/InAs nanoring

Gu Li-Ying,Li Yan-Fang,Chu Wei-Dong,Wei Ying-Hui

Chin. Phys. B, 2012, 21 (**3**): 037301. DOI: 10.1088/1674-1056/21/3/037301

A simple method to synthesize worm-like AlN nanowires and its field emission studies*

Qi Liang(梁琦), Meng-Qi Yang(杨孟骐), Chang-Hao Wang(王长昊), and Ru-Zhi Wang(王如志)†

Institute of New Energy Materials and Devices of Faculty of Materials and Manufacturing, Key Laboratory of Advanced Functional Materials of Education Ministry of China, Beijing University of Technology, Beijing 100124, *China*

(Received 18 December 2020; revised manuscript received 25 January 2021; accepted manuscript online 7 February 2021)

The worm-like AlN nanowires are fabricated by the plasma-enhanced chemical vapor deposition (PECVD) on Si substrates through using Al powder and N_2 as precursors, CaF_2 as fluxing medium, Au as catalyst, respectively. The as-grown worm-like AlN nanowires each have a polycrystalline and hexagonal wurtzite structure. Their diameters are about 300 nm, and the lengths are over 10 μm. The growth mechanism of worm-like AlN nanowires is discussed. Hydrogen plasma plays a very important role in forming the polycrystalline structure and rough surfaces of worm-like AlN nanowires. The worm-like AlN nanowires exhibit an excellent field-emission (FE) property with a low turn-on field of 4.5 V/μm at a current density of 0.01 mA/cm^2 and low threshold field of 9.9 V/μm at 1 mA/cm^2. The emission current densities of worm-like AlN nanowires each have a good stability. The enhanced FE properties of worm-like AlN nanowires may be due to their polycrystalline and rough structure with nanosize and high aspect ratio. The excellent FE properties of worm-like AlN nanowires can be explained by a grain boundary conduction mechanism. The results demonstrate that the worm-like AlN nanowires prepared by the proposed simple and the PECVD method possesses the potential applications in photoelectric and field-emission devices.

Keywords: worm-like aluminum nitride nanowires, growth mechanism, plasma enhanced chemical vapor deposition, field-emission property

PACS: 73.61.Ey, 73.90.+f, 81.05.–t, 81.07.Gf **DOI:** 10.1088/1674-1056/abe3e7

1. Introduction

Aluminum nitride (AlN), a direct wide band gap (6.2 eV) semiconductor, is a potential semiconductor material with a wide range of applications in ultraviolet (UV) photodetectors,[1–3] deep ultraviolet light emitting diode (LED),[4–6] field-emission (FE) devices,[7] surface acoustic wave devices[8,9] due to wide band gap, excellent thermal conductivity, small negative electron affinity ($\leq$ 0.6 eV), and low work function (3.7 eV).[10,11] In addition, AlN can be used in high-power/high- frequency devices because of good reliability and chemical stability.[12] In recent years, AlN has aroused widely research interest out of applications in optoelectronics and electronic fields.

One-dimensional (1D) AlN nanomaterials are one of significant and promising materials due to their nanosizes, large aspect ratios and quantum confinement effects.[13] The AlN nanowires are most widely employed in nano-electronic and nano-optoelectronic devices. In recent years, the AlN nanowires have been successfully fabricated by many methods, including simple chemical vapor deposition (CVD),[11,14–16] physical vapor reaction (PVT),[12] metal–organic chemical vapor deposition (MOCVD),[17] halide vapor-phase epitaxy (HVPE),[18] molecular beam epitaxy (MBE),[4,19,20] and solid phase reaction method.[21] For instance, Cimalla *et al.*[17] obtained AlN nanowires by MOCVD method through using Ni and Au as catalyst. Zhao *et al.*[4] reported that AlN nanowire grown by MBE has excellent optical property. However, the equipment is employed in these researches is complex and expensive, which restricts the widespread application of AlN nanowires.

In order to conquer this disadvantage, some researchers have made extensive efforts to fabricate AlN nanowires by simple method, such as CVD. For example, Chen *et al.*[11] reported the AlN nanowires grown on graphite substrate by simple CVD method through using $AlCl_3$ and NH_3 as aluminum source and nitrogen sources, respectively. Teker[14] reported that AlN nanowires grown on Si substrate by simple CVD method using Al powder and NH_3 as aluminum source and nitrogen sources, respectively. Similarly, Wu and Peng[15] fabricated single-crystalline AlN nanowires by the CVD method through using Al powder and NH_3 as an aluminum source and a nitrogen source, respectively. In addition, Yu *et al.*[16] obtained AlN nanowires by the CVD method through using CaF_2 as a fluxing medium and NH_3 as a nitrogen source. However, NH_3, as a nitrogen source, is unsafe, toxic or corrosive in the CVD method.

Thus, Wang *et al.* reported single crystalline GaN nanowires fabricated by plasma-enhanced chemical vapor deposition (PECVD) through using GaN powder as precursor[22] single crystalline GaN nanowires have also been prepared on a Si substrate by the PECVD through using Au as cat-

*Project supported by the National Natural Science Foundation of China (Grant Nos. 11774017 and 51761135129).

†Corresponding author. E-mail: wrz@bjut.edu.cn

© 2021 Chinese Physical Society and IOP Publishing Ltd

alyst, Ga and N_2 as precursors.[23] Furthermore, we investigate the effect of H_2 gas on the microstructure of GaN nanowires obtained by using Au as catalyst, Ga_2O_3 and N_2 as precursors.[24] In addition, we have been grown polycrystalline GaN nanowires on graphite by the PECVD without catalyst through using Ga and N_2 as precursors.[25] Moreover, single GaN nanowires have been prepared on Al_2O_3 substrate by the PECVD without catalyst through using Ga and N_2 as precursors.[26] However, worm-like AlN nanowires with polycrystalline structure are prepared by the PECVD method through using Al and N_2 as precursors, which have rarely been reported in previous researches.

In this work, we fabricated worm-like AlN nanowires with polycrystalline structure on Si substrate by the PECVD method through using non-toxic raw materials. The N_2 and Al powder are employed as precursors. The reaction temperature is controlled at 1100 °C. The effect of H_2 on morphology of AlN nanowires is studied. The AlN nanorods are obtained without using the H_2 flow. Meanwhile, the growth mechanism of polycrystalline worm-like AlN nanowires is also discussed in detail. Furthermore, the FE properties of polycrystalline worm-like AlN nanowires are studied.

2. Experiments

The worm-like AlN nanowires were fabricated on Si substrates by the PECVD method in a tube furnace through using Al (Alfa, purity 99.999%) and N_2 gas (purity 99.999 %) as precursors. A silicon substrate was placed on the top of the source. The heating rate was 20 °C/min and the flow of Ar gas (purity 99.999%) was 50 sccm. Then, N_2 gas was introduced into the tube furnace for the growth of worm-like AlN nanowires at 1100 °C. During the growth, the N_2 flow rate was maintained at 40 sccm, and the radio frequency (RF) generator worked at 100 W for 2 h. After that, RF generator was shut off and the tube furnace cooled down to room temperature in Ar flow. Finally, a gray product was observed on the Si substrate.

Phases of the as-prepared samples were identified by analyzing the x-ray diffraction (XRD, D8 Advance) through using Cu Ka radiation ($\lambda = 0.154178$ nm). The morphologies of samples were observed by field emission scanning electron microscopy (FESEM; GeminiSEM 300, 5-kV acceleration voltage). The microstructures of samples were studied by high resolution transmission electron microscopy (HRTEM; JEM-2100F, 200-kV acceleration voltage). The binding energies of AlN samples were investigated by x-ray photoelectron spectroscopy (XPS; ESCALAB 250Xi). The Raman spectra of the samples were characterized by Raman spectroscopy (Raman, Renishaw) with 532-nm laser used as an excitation source. Photoluminescence (PL) properties of samples were measured at room temperature by using photoluminescence spectroscopy (Hitachi F-7000).

The FE properties of worm-like AlN nanowires were investigated in a high-vacuum (about 1×10^{-6} Pa) chamber at room temperature. The metal tip was used as an anode, and the worm-like AlN nanowires on the Si substrate were used as a cathode. The distance between the anode and the cathode was 25 μm. High voltage was supplied by a power source (Keithley 248) and current was collected by an electrometer system (Keithley 6514).

3. Results and discussion

3.1. Microstructure analysis

Figure 1 shows the x-ray diffraction pattern of the product fabricated at 1100 °C without and with H_2. According to the standard PDF card, the diffraction peaks at (100), (002), (101), (102), (110), (103), (112), and (201) are identified as those of the wurtzite-type hexagonal AlN (JCPDS card No. 25-1133) with lattice constants of $a = 3.111$ Å and $c = 4.979$ Å. The multi-peak characteristics of XRD patterns indicate that wurtzite-type hexagonal AlN sample has a polycrystalline structure. The diffraction peaks at (111), (220), (311), (400), and (331) are identified as those of Si substrate. No other diffraction peaks from other impurities are found in these samples. The sharp AlN diffraction peaks are observed, which indicate good crystal quality. In addition, we can observe that the the AlN fabricated with H_2 has higher diffraction intensity than AlN fabricated without H_2. It indicates that the AlN fabricated with H_2 has higher crystal quality.

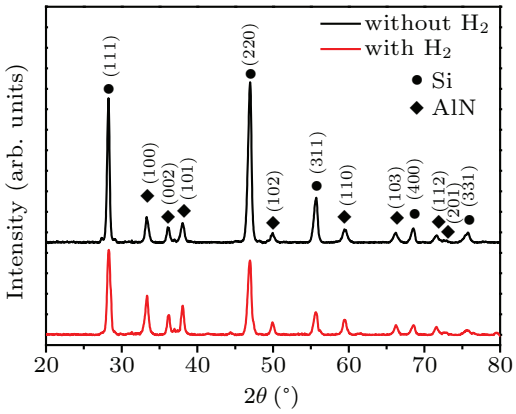


Fig. 1. XRD pattern of products fabricated at 1100 °C without and with H_2.

Figure 2 shows that the TEM images of the products fabricated at 1100 °C. Figures 2(a) and 2(b) show the TEM images of the products fabricated at 1100 °C without H_2. As shown in Fig. 2(b), the HRTEM image reveals hexagonal wurtzite structure of AlN nanomaterials, which is in agreement with the result of XRD. The adjacent spacing of the lattice fringes is measured to be 0.272 nm, which corresponds to the (100) plane of the wurtzite AlN. It indicates that the growth direction of AlN nanomaterials is along the [100] orientation and perpendicular to the (100) crystal plane.[15] Fig-

ures 2(c) and 2(d) show the TEM images of the products fabricated at 1100 °C with H_2. As can be seen from Fig. 2(d), the HRTEM image reveals the hexagonal wurtzite structure of AlN nanowires. The spacing between the adjacent lattice fringes is 0.249 nm. It corresponds to the (002) plane of the wurtzite AlN, which indicates that nanowires are the wurtzite AlN nanowires.[18] The AlN nanowire is 300 nm in diameter and the surface of the AlN nanowire is rough as shown in Fig. 2(c).

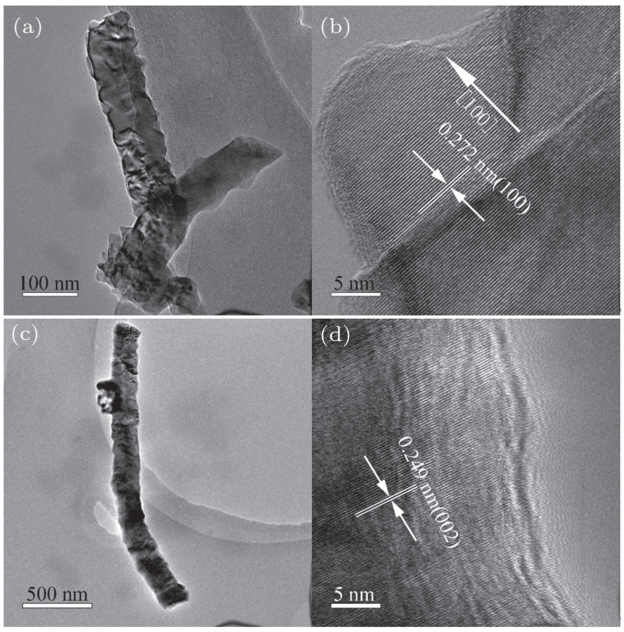


Fig. 2. TEM images of products fabricated at 1100 °C without ((a), (b)) and with ((c), (d)) H_2.

Figure 3 displays the FESEM images of the products fabricated at 1100 °C. The FESEM image of the product fabricated at 1100 °C without H_2 is shown in Fig. 3(a). The AlN nanorods are obtained. The AlN nanorods are 4 μm–8 μm in length and 300 nm–700 nm in diameter. When H_2 is introduced into the reaction (Fig. 3(b)), the products of sample are worm-like AlN nanowires. The worm-like AlN nanowires have diameters in a range of 300 nm–500 nm and lengths of 10 μm. The surfaces of worm-like AlN nanowires are rough, which are consistent with the result of TEM. Figure 3 shows the uniform distribution of products over the area under observation. The results of Figs. 2 and 3 indicate that introduction of H_2 has a significant effect on the morphologies and growths of AlN nanomaterials.

Figure 4 shows Raman spectra of AlN nanomaterials fabricated at 1100 °C with and without H_2. Raman active modes are observed at 661 cm^{-1} and 658 cm^{-1} for the two samples respectively, which can be assigned to the E_2 (high) phonon modes of wurtzite AlN. Comparing the position of E_2 (high) phonon peak for bulk AlN (657.4 cm^{-1}),[27] the minor shift of 0.6 cm^{-1} is revealed in Raman spectra of worm-like AlN nanowires fabricated at 1100 °C with H_2. It indicates that a negligible compressive stress exists in the lattice of worm-like AlN nanowires.[28] The Raman peak at 524 cm^{-1} originates from the silicon substrate. In our study, the Raman peak with minor shift implies the good crystal quality.[15]

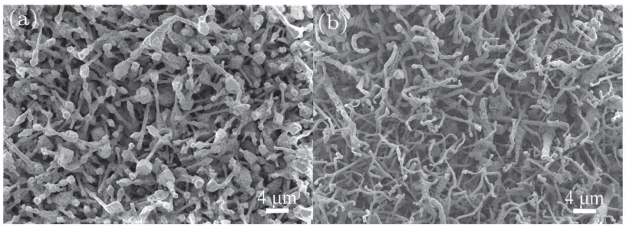


Fig. 3. FESEM images of products fabricated at 1100 ° without (a) and with (b) H_2.

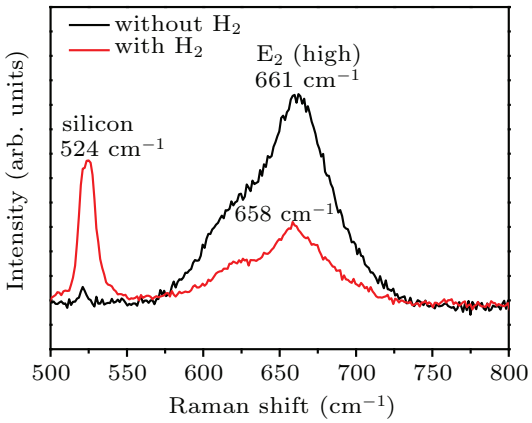


Fig. 4. Raman spectra of AlN nanomaterials fabricated at 1100 °C.

Figure 5 shows the XPS spectra of worm-like AlN nanowires fabricated at 1100 °C with H_2. Figure 5(a) shows a survey spectrum of worm-like AlN nanowires from 0 eV to 700 eV and the XPS peaks are assigned to the main components of Al, C, N, and O, indicating the presence of elemental Al and N. As shown in Figs. 5(b) and 5(c), the binding energies of Al 2p and N 1s are centered at 73.5 eV and 396.7 eV respectively, which are consistent with the reported values of bulk AlN from the literature.[18] Quantification of the Al 2p peak and N 1s peak gives an average Al/N atomic ratio of 1.334:1. It indicates a little nitrogen-deficient or oxygen impurity existing in worm-like AlN nanowires.[29] The Ca and F elements originate from extrinsic contaminations of CaF source.

Figure 6 displays the room temperature PL spectrum of worm-like GaN nanowires fabricated at 1100 °C with H_2. A wide emission band ranging from 350 nm to 520 nm centered at 438 nm corresponding to the blue region is observed. Obviously, this emission does not originate from the direct bandgap emission. The PL mechanism of bule emission band of AlN nanomaterials has been studied in some literature.[7,13,30–33] The results reveal that the broad bule band originates from the vacancy of N, Al or O impurity, but without giving detailed explanation. For example, Wu *et al.* demonstrated the blue emission centered at 452 nm originates from the oxygen deep level and the radiative recombination of a photogenerated hole

with an electron occupying the nitrogen vacancy.[30] Shen *et al*. reported that the blue emission band centered at 446 nm can be attributed to a donor–acceptor pair transition, involving O_N, V_N (nitrogen vacancy), and O_N–V_{Al} complex defect centers.[7] In our work, the broad blue band can be assigned to nitrogen-deficient condition or oxygen impurity of worm-like AlN nanowires, which is confirmed by XPS analysis. We infer that some oxygen atoms occupy the sites of N as deep level, and a majority of O atoms adsorb on the surfaces of AlN nanowires as surface impurities.[29]

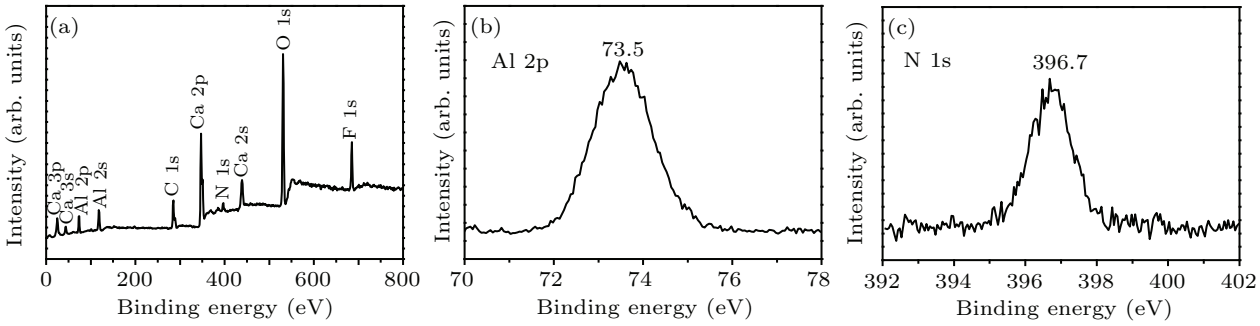


Fig. 5. XPS spectra of worm-like AlN nanowires fabricated at 1100 °C with H_2: (a) general scan spectrum, (b) Al 2p band, and (c) N 1s band.

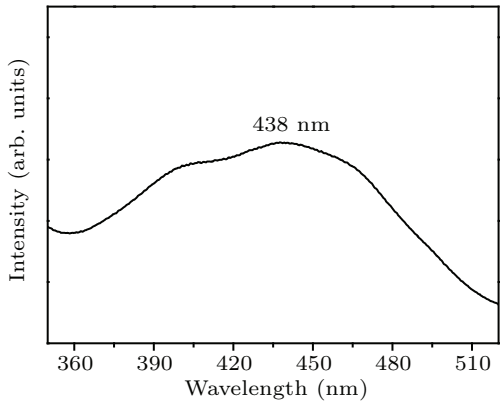


Fig. 6. PL spectrum of worm-like GaN nanowires fabricated at 1100 °C with H_2.

3.2. Growth mechanism

For the growth of worm-like AlN nanowires, firstly, H_2 and N_2 are ionized by coupling with radio frequency (RF), then N and H plasmas are formed. Secondly, Al powders are transformed into Al gas (*i.e*. gasified Al) at high temperature. Thirdly, the reaction of gaseous Al with ionized nitrogen plasma results in the formation of crystalline AlN. Meanwhile, H plasma enters into the crystalline AlN lattice to tailor AlN microstructure and morphology. Finally, worm-like AlN nanowires formed. Thus, the reaction can be expressed as follows:

$$N_2 \rightarrow N^*, \tag{1}$$

$$H_2 \rightarrow H^*, \tag{2}$$

$$N^* + Al \rightarrow AlN. \tag{3}$$

In our work, the growth of worm-like AlN nanowires follows the vapor–liquid–solid (VLS) mechanism. In the growth process, the Au layer on the Si substrate transforms into Au droplets under high temperature firstly. Then, H, N plasma, and gaseous Al are dissolved into Au droplets. The N plasma reacts with Al atoms to form crystalline AlN and nucleates. With the formation of AlN at interface between AlN nucleus and Au droplets, AlN nanowires form by the growth of AlN nucleus. The H plasma enters into the crystalline AlN nanowires' lattices to restrict the bonding between Ga and N because H plasma bonds with N more easily.[34,35] Thus, there are atomic dislocation and defects in the lattices. At high temperature, the grain boundaries are formed by the rearrangement of the atoms in the AlN nanowires. However, the AlN nanowires still are surrounded by H plasma atmosphere. Finally, worm-like AlN polycrystalline nanowires with rough surface are formed due to the etch of H plasma at the surface of AlN nanowires.[36] Figure 7 shows the growth mechanism diagram of worm-like AlN nanowire, i.e. the growing process for worm-like AlN nanowire from step (a) to step (f).

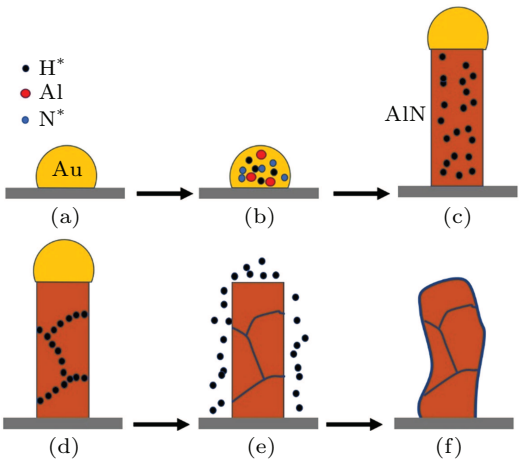


Fig. 7. (a)–(f) Growing processes for worm-like AlN nanowire.

4. Field-emission property

The FE curve of current density (J) *versus* applied electric field (E) of worm-like AlN nanowires is presented in Fig. 8(a). By definition, the turn-on field (E_{to}) and the threshold field (E_{thr}) are the electric fields required to produce a current density of 10 μA/cm^2 and 1 mA/cm^2, respectively, which can

satisfy the primary requirement for applications in the conventional flat panel displays.[11] The (E_{to}) and the (E_{thr}) of 4.5 V/μm and 9.9 V/μm, respectively, are obtained for worm-like AlN nanowries. The E_{to} of worm-like AlN nanowires is comparable to the reported values of AlN nanowires[37] and nanotip array.[38] The reason for the low turn-on electric field and high FE current density are probably due to polycrystalline and rough structure and the nanosize of the emitter materials.[38–40] In order to better understanding the field-emission behavior, the relationship between current density J and applied electric field E can be analyzed by using a simplified Fowler–Nordheim (FN) equation[41]

$$\ln\left(\frac{J}{E^2}\right) = \ln\left(\frac{\alpha A\beta^2}{\phi}\right) - \frac{B\phi^{3/2}}{\beta E}, \tag{4}$$

where $A = 1.54 \times 10^{-6}$ (A·eV·V^{-2}), $B = 6.83 \times 10^3$ (eV$^{-3/2}$·V·μm^{-1}), E is the applied electric field, ϕ is the work function of the emitting materials, β is the field enhancement factor, and α is the effective emission area. Figure 8(b) shows the corresponding FN plot. Given the slope and intercept of the $\ln(J/E^2)$ *versus* $1/E$ plot, the field enhancement factor β and the effective emission area α can be calculated if work function of the emitting material is known. The FN plot of worm-like AlN nanowires is linear in high-field region, which indicates the tunneling behavior of AlN semiconductor and the field emission caused by vacuum tunneling. If effective emission area α is 1, the field enhancement factor β is the geometric field enhancement factor. The geometric field enhancement factor is proportional to the curvature of emitting material. According to the estimate of the curvature of worm-like AlN nanowires, the geometric field enhancement factor is 40–200. Based on the reported value of work function of AlN (3.7 eV), the calculated β value of worm-like AlN nanowires is 1442. However, the calculated β value of worm-like AlN nanowires is greater than the geometric field enhancement factor. Because the intrinsic β of nanowires is not only dependent on their density, uniformity, and the geometrical feature, including the radius of curvature and the aspect ratio of l/r, where l and r are the length and radius of nanowire, respectively,[11,18] but also related closely to the effective emission area α. The result indicates that the effective emission area α is greater than 1. In our work, efficient field emission from worm-like AlN nanowires is attributed mainly to high aspect ratio, the uniformity and effective emission area of worm-like AlN nanowires. The effective emission area is related to the microstructure of worm-like AlN nanowires. As seen from Fig. 1 the AlN polycrystalline structure is very important for the electron transport of worm-like nanowires.

The electron transport can be mainly influenced by the microstructure of material. However, the electron supply can be dependent on the electron transport. Thus, such a low E_{to} value for worm-like polycrystalline AlN nanowires is explained by a nanocrystalline electron transport and grain boundary conduction mechanism.[41] We suggest that the conducting channels can depend on the polycrystalline structure. The grain boundaries of AlN nanocrystals in worm-like AlN nanowires act as effective conduction channels. The electron can traverse across the worm-like AlN nanowires from the conduction channels. The electron emission occurs from the region of the grain boundary defects, which is responsible for the increasing of effective emission area, resulting in high emission performance.[39,41] Figure 8(c) shows the filed-emission (FE) stability of worm-like AlN nanowires. The average current density is estimated to be 100 μA/cm^2. The emission current density tends to be stable approximately with the fluctuation of about 50% for 60 min. The fluctuation of the current density can be explained by the absorption and desorption of molecules at the rough surfaces of polycrystalline worm-like AlN nanowires in vacuum chamber during electron emission.[11] In addition, the fluctuation of the current density can be influenced by the mechanical vibration which results in the distance fluctuations between the anode and the cathode. At the testing time of 60 min, no significant degradation is observed, which demonstrates high stability of field emission of polycrystalline AlN nanowires.

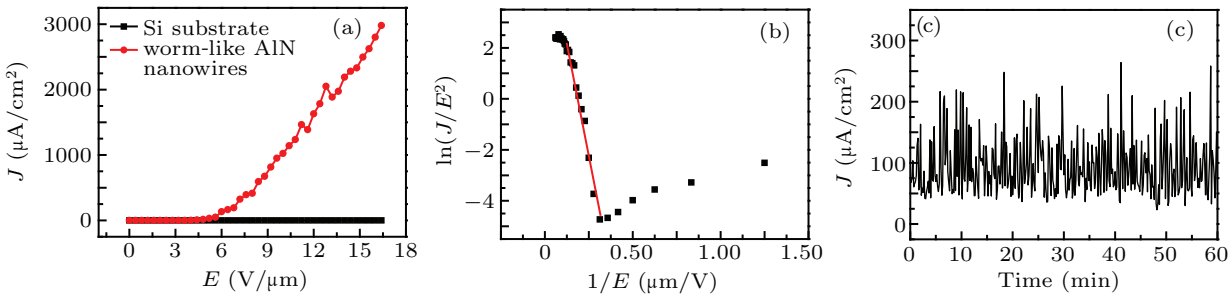


Fig. 8. (a) Field-emission current density (J) *versus* applied electric field (E) for worm-like AlN nanowires and substrate. (b) Flowler–Nordheim plot of the $\ln(J/E^2)$ *versus* $1/E$. (c) Field-emission stability of worm-like AlN nanowires.

5. Conclusions

In summary, the worm-like AlN nanowires have been prepared by a simple and green PECVD method through using non-toxic precursors. The worm-like AlN nanowires exhibit rough surfaces and uniformity. The worm-like AlN nanowires are polycrystalline and belong to hexagonal wurtzite structure.

The worm-like AlN nanowires is grown by the VLS mechanism. Hydrogen plasma plays an important role in the forming of polycrystalline structure and rough surface of worm-like AlN nanowires. Hydrogen plasma enters into the crystalline AlN nanowires' lattices to restrict the bonding brtween Ga and N. The PL result indicates that a blue emission band centered at 438 nm is observed, which corresponds to the deep-level or trap-level emission. The worm-like AlN nanowires show a good field emission property with a low turn-on field of 4.5 V/μm and low threshold field of 9.9 V/μm. The excellent FE property is due to the polycrystalline and rough structures of worm-like AlN nanowires with nanosize and high aspect ratio. In addition, the emission current density of worm-like AlN nanowires exhibits high stability. Thus, the proposed method shows a simple and green technical way of fabricating the polycrystalline AlN nanowires with potential applications in optoelectronic and field-emission devices.

References

[1] Zheng W, Huang F, Zheng R and Wu H 2015 *Adv. Mater.* **27** 3921
[2] Liu F, Li L F, Guo T Y, Gan H B, Mo X S, Chen J, Deng S Z and Xu N S 2012 *Nanoscale Res. Lett.* **7** 454
[3] Ali Y A and Teker K 2019 *Microelectron. Eng.* **211** 26
[4] Zhao S, Djavid M and Mi Z 2015 *Nano Lett.* **15** 7006
[5] Laleyan D A, Zhao S, Woo S Y, Tran H N, Le H B, Szkopek T, Guo H, Botton G A and Mi Z 2017 *Nano Lett.* **17** 3738
[6] Mi Z, Zhao S, Woo S Y, Bugnet M, Djavid M, Liu X, Kang J, Kong X, Ji W, Guo H, Liu Z and Botton G A 2016 *J. Phys. D: Appl. Phys.* **49** 364006
[7] Shen L, Lv W, Wang N, Wu L, Qi D, Ma Y and Lei W 2017 *CrystEngComm* **19** 5940
[8] Redkin A N, Yakimov E E, Roshchupkin D V and Korepanov V I 2019 *Thin Solid Films* **684** 15
[9] Pandey A, Kaushik J, Dutta S, Kapoor A K and Kaur D 2018 *Thin Solid Films* **666** 143
[10] Kurtuldu F, G?k?e A and Kurt A O 2018 *J. Mater. Sci: Mater. El.* **29** 20688
[11] Chen F, Ji X and Zhang Q 2015 *J. Alloys Compd.* **646** 879
[12] Wang G, Chen C, Shao Y, Chen F, Zhang L, Wu Y and Hao X 2019 *J. Alloys Compd.* **794** 171
[13] Zheng M, Jia Q, Liu X and Jia G 2019 *Ceram. Int.* **45** 12387
[14] Teker K 2015 *Mater. Sci. Technol.* **31** 1832
[15] Wu H M and Peng Y W 2015 *Ceram. Int.* **41** 4847
[16] Yu L, Lv Y, Zhang X, Zhang Y, Zou R and Zhang F 2011 *J. Cryst. Growth* **334** 57
[17] Cimalla V, Foerster C, Cengher D, Tonisch K and Ambacher O 2006 *Phys. Status Solidi B* **243** 1476
[18] Byeun Y K, Telle R, Jung S H, Choi S C and Hwang H I 2010 *Chem. Vapor Depos.* **16** 72
[19] Zhao S, Connie A T, Dastjerdi M H, Kong X H, Wang Q, Djavid M, Sadaf S, Liu X D, Shih I, Guo H and Mi Z 2015 *Sci. Rep.* **5** 8332
[20] E Y X, Hao Z, Yu J, Wu C, Liu R, Wang L, Xiong B, Wang J, Han Y, Sun C and Luo Y 2015 *Nanoscale Res. Lett.* **10** 383
[21] Aghdaie A, Haratizadeh H, Mousavi S H, Jafari Mohammadi S A and de Oliveira P W 2015 *Ceram. Int.* **41** 2917
[22] Wang Y Q, Wang R Z, Li Y J, Zhang Y F, Zhu M K, Wang B and Yan H 2013 *CrystEngComm* **15** 1626
[23] Zhao J W, Zhang Y F, Li Y H, Su C H, Song X M, Yan H and Wang R Z 2015 *Sci. Rep.* **5** 17692
[24] Ji Y H, Wang R Z, Feng X Y, Zhang Y F and Yan H 2017 *J. Phys. Chem. C* **121** 24804
[25] Feng X Y, Wang R Z, Liang Q, Ji Y H and Yang M Q 2019 *Cryst. Growth Des.* **19** 2687
[26] Liang Q, Wang R Z, Yang M Q, Wang C H and Liu J W 2020 *Acta Phys. Sin.* **69** 087801 (in Chinese)
[27] Davydov V Y, Kitaev Y E, Goncharuk I N and Smirnov A N 1998 *Phys. Rev. B* **58** 12899
[28] Liang Q, Wang R Z, Yang M Q, Ding Y and Wang C H 2020 *Thin Solid Films* **710** 138266
[29] Lei M, Yang H, Guo Y F, Song B, Li P G and Tang W H 2007 *Mater. Sci. Eng. B* **143** 85
[30] Wu Q, Zhang F, Wang X Z, Liu C and Hu Z 2007 *J. Phys. Chem. C* **111** 12639
[31] Xu C K, Xue L, Yin C R and Wang G H 2003 *Phys. Status Solidi A* **198** 329
[32] Yu L, Hu Z, Ma Y, Huo K, Chen Y, Sang H, Lin W and Lu Y 2007 *Diam. Relat. Mater.* **16** 1636
[33] Zhang F, Wu Q, Wang X B, Liu N, Yang J, Hu Y M, Yu Le S, Wang X Z, Hu Z and Zhu J M 2009 *J. Phys. Chem. C* **113** 4053
[34] Yeh Y H, Chen K M, Wu Y H, Hsu Y C, Yu T Y and Lee W I 2011 *J. Cryst. Growth* **333** 16
[35] Sprenger J K, Cavanagh A S, Sun H, Wahl K J, Roshko A and George S M 2016 *Chem. Mater.* **28** 5282
[36] Yeh Y H, Chen K M, Wu Y H, Hsu Y C and Lee W I 2011 *J. Cryst. Growth* **314** 9
[37] Liu F, Su Z J, Mo F Y, Li L, Chen Z S, Liu Q R, Chen J, Deng S Z and Xu N S 2011 *Nanoscale* **3** 610
[38] Tang Y, Cong H, Chen Z and Cheng H 2005 *Appl. Phys. Lett.* **86** 233104
[39] Obraztsov A N, Volkov A P and Pavlovski I Y 1998 *J. Exp. Theor. Phys. Lett.* **68** 59
[40] Dinh D V, Kang S M, Yang J H, Kim S W and Yoon D H 2009 *J. Cryst. Growth* **311** 495
[41] Zhao W, Wang R Z, Song Z W, Wang H, Yan H and Chu P K 2013 *J. Phys. Chem. C* **117** 1518